216493: Your manuscript has been accepted

From: Rama B. Bhat <aav@hindawi.com>
To: its_ahmadyusuf@yahoo.com
Cc: rbhat@alcor.concordia.ca, azma.putra@utem.edu.my, roszaidi@utem.edu.my, razali@utem.edu.my, sajidin@student.utem.edu.my
Date: Friday, 26 July, 2013 8:24:41 PM
Subject: 216493: Your manuscript has been accepted

Dear Dr. Yusuf Ismail,

The review of the Research Article 216493 titled "Normal incidence of sound transmission loss of a double-leaf partition inserted with a micro-perforated panel," by Ahmad Yusuf Ismail, Azma Putra, Roszaidi Ramlan, Md Razali Ayob and Muhammad Sajidin Py submitted to Advances in Acoustics and Vibration, has been completed, and I am pleased to inform you that your manuscript has now been accepted for publication in the journal.

The publication process of your manuscript will be initiated upon the receipt of the electronic files. Please login to the Manuscript Tracking System at the link below using your username and password, and upload the electronic files of your final accepted version within the next 2-3 days.

http://mts.hindawi.com/author/216493/upload.files/

The electronic files should include the following:

1- Source file (Word or TeX/LaTeX).
2- Final PDF file of the accepted manuscript.
3- Editable Figure files (each figure in a separate eps/postscript/word file) if any, taking into consideration that tiff, jpg, jpeg, bmp formats are not editable.

Thank you again for submitting your manuscript to Advances in Acoustics and Vibration.

Best regards,

Rama B. Bhat
rbhat@alcor.concordia.ca

Advances in Acoustics and Vibration

Articles in Press [2 articles]

Normal incidence of sound transmission loss of a double-leaf partition inserted with a micro-perforated panel

A. Y. Ismail, A. Putra*, R. Ramlan, Md. R. Ayob, M. S. Py

Faculty of Mechanical Engineering, Universiti Teknikal Malaysia Melaka
Hang Tuah Jaya, Durian Tunggal Melaka 76100, Malaysia

Abstract

A double-leaf partition in engineering structures has been widely applied for its advantages i.e. in terms of its mechanical strength as well as its lightweight property. In noise control, the double-leaf also serves to be an effective noise barrier. Unfortunately at low frequency, the sound transmission loss reduces significantly due to the coupling between the panels and the air between them. This paper studies the effect of a micro-perforated panel (MPP) inserted inside a double-leaf partition on the sound transmission loss performance of the system. The MPP insertion is proposed to provide a hygienic double-leaf noise insulator replacing the classical abrasive porous materials between the panels. It is found that the transmission loss improves at the troublesome mass-air-mass resonant frequency if the MPP is located closer to the solid panel. The mathematical model is derived for normal incidence of acoustic loading.

Key words: Double-leaf, partition, micro-perforated panel, transmission loss

1. Introduction

A double-leaf structure is a common structural design for many engineering applications. The vehicle body such as in cars, trains and airplanes, as well as the walls of a building are some examples of double-leaf partition in practice. From the acoustical engineering point of view, the double-leaf is proposed to be a better noise barrier compared to the single-leaf. However, there remains a problem on the double-panel which is the weak sound transmission loss (STL) performance at low frequency due to the 'mass-air-mass' resonance. This causes the double-leaf loses its superiority over the single-leaf [1].

*Corresponding author. Tel.:+606 234 6720; fax:+606 234 6884.
Email address: azma.putra@utem.edu.my (A. Putra)

Several works have been established to solve this problem. This includes employing an absorbtive materials inside the gap of a double-leaf e.g. fiberglass [2] and rockwool [3] which can effectively increase the STL due to additional damping to the air layer provided by the absorbent. Mao and Pietrzko [4] proposed a technique by installing the Hemholtz resonators at the air gap. The resonator acts like single-degree of freedom system of which its natural frequency depends on its geometry. In order to increase the STL at mass-air-mass resonance, the Hemholtz resonator is tuned to the same resonant frequency. Li and Cheng [5] used an active control system to control the acoustic modes in the gap by using a sound source and an actuator. The sound source reduces the transmission energy by suppressing certain acoustic modes in the air gap while the actuator reduces energy from the structural path by creating counter forces on the two panels to suppress the vibration. Similarly, Li *et al.* [6] used a long T-shaped resonators embedded along the edge of the double-panel. This is also aimed to actively control both acouctics and structural path in the gap. It is found that by varying the location of the resonators the STL at resonance can be significantly improved. Mahjoob *et.al.* [7] introduced the newtonian fluids to control the acoustic path inside the gap. Air, oil and ferromagnetic nano-particle fluid were used as a filler between the two panels. Although not practical, this method is also shown to increase the STL at resonance.

However, use of acoustic absorbers, such as foam or fibrous type materials inside a double-panel are still the most cheapest and common practice to increase the sound insulation performance [2, 3]. For noise control application where abrasive and polluting materials cannot be presented, such as in the food industry where hygienic condition is critical to be maintained around the processing machines, conventional synthetic fibrous materials are thus not the solution. Although it is hidden between the panels, a noise barrier panel which is easy to be cleaned, handled and is free from hazardous substances to health is therefore necessary.

An alternative fiber-free absorber which has gained more popularity is a micro-perforated panel (MPP) absorber. MPP is a perforated panel with millimetric size holes backed by air cavity and rigid surface found by Dah You Maa in 1975. The hole diameter must be in the range between $0.05-1$ mm and the perforation ratio between $0.5-1.5\%$ for optimum absorption [8]. As the MPP can be made from panel, it provides several advantages such as non-fibrous, non-abrasive, non-polluting and safer in case of fire hazard. Although the MPP is mainly applied for sound absorber, several works have also been published concerning its sound insulation performance.

Dupont *et al.* [9] investigated the sound transmission loss of a double-leaf structure where a MPP is backed by a solid panel. Toyoda and Takahashi [10] studied the sound transmission loss of a MPP by subdividing the air cavity behind the MPP to have the sound propagation in normal incidence in the cavity. The transmission loss is found to increase at mid-frequencies. Most recently, models of sound transmission loss for a multi-layer partition with a MPP are proposed by Mu *et al.* [11]. In their model, the MPP is located at the outer layer of the system.

In this paper, similar multi-layer structure is proposed, but with the MPP inserted between two solid plates. Apart for hygienic purposes, the application can also be found for example a multi-layer window system where a transparent panel is required to improve the noise insulation. The next section describes the derivation of the mathematical model and presents the simulation results of the effect of the MPP insertion, in terms of its location in the gap as well as its hole size and perforation ratio, on the sound transmission loss. The derivation is conducted only for the sound field with normal incidence. Recent finding suggests that the effect of mass-air-mass resonance for an infinite double-panel system subjected to the diffuse field incidence is not correct due to the internal resonance in the cavity in the direction parallel to the panel [12]. Numerical modelling technique is required, but this is beyond the scope of this paper.

2. Governing equations

2.1. Propagating acoustic pressure

A mechanical system of a double-leaf inserted with a MPP (abbreviated here as DL-MPP) under normal incidence of acoustic loading can be seen in Figure 1. The solid panels are separated by distance D and the MPP is located by distance l from the back soild plate. Each of the solid and the MPP panels has mass per unit area M and m, respectively and they are assumed to be supported on identical mountings having stiffness per unit area s and damping constant per unit area r. The incident pressure is expressed as

$$p_i(x) = Ae^{-jkx} \tag{1}$$

and the reflected pressure is given by

$$p_r(x) = Be^{jkx} \tag{2}$$

where $k = \omega/c$ for k represents the acoustic wavenumber, ω is the angular velocity and c is the sound speed in the air. Here and for the rest of the equations, time dependence $e^{j\omega t}$ is implicitly

assumed. At $x = 0$, the acoustic pressure acting on the incident side of the front panel can be written as

$$p_1 = p_i(x = 0) + p_r(x = 0) = A_1 + B_1 \tag{3}$$

In the same way as in Eqs. 1 and 2, the total pressure on the other side of the front panel surface is thus

$$p_2 = A_2 + B_2 \tag{4}$$

The relation between the average surface particle velocity $\bar{v}$ and the sound pressure exciting the panel can be obtained by using Euler equation $\bar{v} = -1/j\rho\omega(\mathrm{d}p/\mathrm{d}x)$ [13]. For both surfaces of each panel, at $x = 0$ for the front panel this gives

$$z_f v_{p_1} = A_1 - B_1 \tag{5}$$

$$z_f v_{p_1} = A_2 - B_2 \tag{6}$$

while at $x = D - l$ for the MPP

$$z_f \bar{v} = A_2 e^{-jk(D-l)} - B_2 e^{jk(D-l)} \tag{7}$$

$$z_f \bar{v} = A_3 e^{-jk(D-l)} - B_3 e^{jk(D-l)} \tag{8}$$

and at $x = D$ for the back panel

$$z_f v_{p_3} = A_3 e^{-jkD} - B_2 e^{jkD} \tag{9}$$

$$p_t = z_f v_{p_3} \tag{10}$$

where v_p is the velocity of the panel, $\bar{v}$ is the mean particle velocity over the MPP surface and $z_f = \rho c$ is the acoustic impedance of air with ρ is the air density. Note that for the solid plate, the mean particle velocity on its surface equals to the velocity of the panel $\bar{v} = v_p$. This is valid for light fluid such as air and not for heavy meadium such as water.

For convenience, the distance between the panel is assumed much smaller compared to the acoustic wavelength ($kD \ll 1$). The cavity pressures can therefore be assumed uniform between each gap

$$p_2 \approx p_3 = A_2 + B_2 = p_b \tag{11}$$

$$p_4 \approx p_5 = A_3 + B_3 = p_c \tag{12}$$

By substituting Eqs. (11) and (12) into Eqs. (7) and (8) yields

$$z_f \bar{v} = A_2 - B_2 - jk(D-l)p_b \tag{13}$$

$$z_f \bar{v} = A_3 - B_3 - jk(D-l)p_c \tag{14}$$

Using the same way to the surface pressure on the back solid panel ($x = D$) gives

$$z_f v_{p_3} = A_3 - B_3 - jkDp_c \tag{15}$$

As the cavity pressure is uniform, Eqs. (5) and (13) can be combined to give

$$p_b = \frac{z_f \left(v_{p_1} - \bar{v}\right)}{jk(D-l)} \tag{16}$$

while for Eqs. (14) and (15) , it yields

$$p_c = \frac{z_f \left(\bar{v} - v_{p_1}\right)}{jkl} \tag{17}$$

2.2. Hole impedance and mean particle velocity

As the acoustic pressure impinges on the MPP, the air particles penetrate the holes and also excite the remaining solid surface of the panel. The combination between the panel velocity and particle velocity inside the holes creates the mean particle velocity given by [14]

$$\bar{v} = v_p \left(1 - \sigma\right) + \sigma v_h \tag{18}$$

where σ is the perforation ratio and v_h is the particle velocity inside the holes. The motion of fluid inside the hole depends on the impedance of the hole which according to Maa [8] is given by

$$Z_o = Z_{o,R} + Z_{o,I} \tag{19}$$

with

$$Z_{o,R} = \frac{32 v_a t}{d_o^2} \left[\left(1 + \frac{X_o^2}{32}\right)^{1/2} + \left(\frac{\sqrt{2} X_o}{8}\right) \frac{d_o}{t} \right] \tag{20}$$

$$Z_{o,I} = -j\rho\omega t \left[1 + \left(9 + \frac{X_o^2}{2}\right)^{-1/2} + \left(\frac{8}{3\pi}\right) \frac{d_o}{t} \right] \tag{21}$$

where $X_o = \left(d_o/2\right) \left(\omega\rho/v_a\right)^{1/2}$, d_o is the hole diameter, t is the plate thickness and v_a is the viscosity of the air, i.e. 1.8×10^{-5} Ns/m^2. The real part of the impedance $Z_{o,R}$ represents the viscous effect responsible for the friction between the inner solid surface of hole and the air and the imaginary

part $Z_{o,I}$ represents the inertia of the air inside the holes of which the air moves like a piston. From these mechanisms, the net pressure Δp on the surface of the MPP can be expressed as [14]

$$Z_{o,R}\left(v_h - v_p\right) + Z_{o,I} v_h = \Delta p \tag{22}$$

Equation (22) can also be re-arranged as

$$v_h - v_p = \frac{\Delta p}{Z_o} - \frac{Z_{o,I}}{Z_o} v_p \tag{23}$$

By substituting this into Eq. (18), the mean particle surface velocity can also be expressed as the function of the net pressure given by

$$\bar{v} = \gamma v_p + \frac{\sigma \Delta p}{Z_o} \tag{24}$$

where $\gamma = 1 - (\sigma Z_{o,I}/Z_o)$ is the complex non-dimensional terms.

2.3. Sound transmission loss

The equation of motion for the solid back panel is given by

$$z_{p_3} v_{p_3} = p_c - p_t \tag{25}$$

where $z_{p_3} = z_{p_1} = j\omega M + r - js/\omega$ is the mechanical impedance of the panel. The damping constant can be written as $r = \omega_n \eta M$ with $\omega_n = (s/M)^{1/2}$ the natural frequency of the system and η the damping loss factor. Substituting Eqs. (10), (17) and (24) into Eq. (25) then dividing both sides with v_{p_3} yields the panel velocity ratio

$$\frac{v_{p_2}}{v_{p_3}} = \frac{1 + jkl\left(1 + \dfrac{z_{p_3}}{z_f}\right)}{\gamma + \dfrac{z_{p_2}}{Z}} \tag{26}$$

The equation of motion for the MPP is expressed as

$$z_{p_2} v_{p_2} = \Delta p \tag{27}$$

where $z_{p_2} = j\omega m + r - js/\omega$. Substituting Eqs. (16), (17) and (24) into Eq. (27) and again dividing both side with v_{p_3} yields

$$\frac{v_{p_1}}{v_{p_3}} = \frac{\left(jk(D-l)\dfrac{z_{p_2}}{z_f}\right)\left[1 + jkl\left(1 + \dfrac{z_{p_3}}{z_f}\right)\right] + \left(\gamma + \dfrac{z_{p_2}}{Z}\right)\left[1 + jkD\left(1 + \dfrac{z_{p_3}}{z_f}\right)\right]}{\gamma + \dfrac{z_{p_2}}{Z}} \tag{28}$$

It can be seen that the velocity ratio of the solid panels depends on the location of the MPP inside the gap. From the equation of motion of the front solid panel

$$z_{p_1} v_{p_1} = p_1 - p_b \tag{29}$$

and using the relation between incident and reflected pressure in Eqs. (3) and (5) gives

$$z_{p_1} v_{p_1} = 2p_i - z_f v_{p_1} - \frac{z_f \left(v_{p_1} - \bar{v}\right)}{jk(D-l)} \tag{30}$$

By dividing both side with $p_t = z_f v_{p_3}$, the ratio of the incident and reflected pressure is given by

$$\frac{p_i}{p_t} = \frac{1}{j2k(D-l)} \left(\frac{v_{p_1}}{v_{p_3}} \left[1 + jk(D-l) \left(1 + \frac{z_{p_1}}{z_f} \right) \right] - \frac{v_{p_2}}{v_{p_3}} \left(\gamma + \frac{z_{p_2}}{Z} \right) \right) \tag{31}$$

As for plane wave, the sound power W is proportional to the sound intensity I which is simply a ratio of squared magnitude sound pressure to the air impedance, $I = \left|p^2\right| / z_f$. The transmission coefficient is therefore written as

$$\tau = \left| \frac{p_t}{p_i} \right|^2 \tag{32}$$

and the transmission loss in dB unit is

$$\mathrm{STL} = 10 \log_{10} \left(\frac{1}{\tau} \right) \tag{33}$$

3. Analytical results

3.1. Effect of MPP location, hole diameter and perforation ratio

Figure 2 shows the transmission loss under normal incidence of acoustic loading for double-leaf (DL) [1], triple-leaf (TL) and double-leaf with MPP (DL-MPP) located exactly at the middle of the solid panels ($l = 0.5D$). All three panels have the same thickness of 1 mm made of aluminium (density 2700 kg/m^3) with air gap $D = 100$ mm between the solid plates. Throughout the paper, the stiffness per unit area of the mounting used in the calculation is $s = 100$ N/m^3 and the damping loss factor is $\eta = 0.01$. The graph is plotted from 50 Hz to 1 kHz to have better clarity around the resonance as well as for ease of analysis. The 'mass-air-mass' resonance of the DL can be seen to occur around 170 Hz shown by the 'drop' value of STL to 0 dB; a well-known phenomenon which occurs when the panels moves out-of-phase. It can also be seen that inserting another solid panel between the double-panels (TL) yields the second resonance at 280 Hz corresponding to

the gap between the middle and the back panel. This can be considered to worsen the problem although the STL at mid-high frequency significantly increases due to the increase of mass. The insertion of MPP between the DL (in the middle) overcomes the second resonance. However, the first resonance remain occurs corresponding to the gap of the solid plates.

As the aim is to improve the STL of the conventional double-leaf at the resonance, Figure 3 shows the results for the DL and DL-MPP for different distance l of the MPP to the solid plate. As in Figure 2 the resonance can be seen at 170 Hz for the DL and also for the DL-MPP with MPP at the middle of the gap. The presence of the MPP gives no effect to overcome the resonance in this case.

For other locations of the MPP in Figure 3, as the MPP shifts closer to the solid panel, regardless the front or back solid panel, the STL can be observed to increase at the resonance. The additional damping due to the viscous force in the MPP holes influences the air layer in front of the solid plate which breaks the coupling between the solid panels and the air. It can also be seen that the position of the MPP in the gap also affects the STL at mid to high frequency in this case above 400 Hz. Contrary to the STL at resonance, the STL above the resonance increases as it moves away from the solid panel within halfway of the gap. The effect of MPP to breach the mass-air-mass resonance is also discussed by Mu *et al.* [11] where the MPP is located at the outer layer of the partition system. However, no detailed discussion is presented regarding the gap of the MPP.

Figure 4 shows the effect of hole diameter of MPP to the STL for fixed MPP location, $l = 0.1D$. Around the resonance region up to 400 Hz, decreasing the hole diameter improves the STL as this increases the domination of the real part of the hole impedance which thus provides more viscous force or damping to the MPP.

In Figure 5, the effect of the perforation ratio is investigated. It can be seen that increasing the perforation ratio does not give significant differences to the STL around the resonance. Therefore, to benefit with STL improvement at high frequency due to added mass in the system, the lowest perforation ratio for the MPP, i.e. $\tau = 0.5\%$ is preferred.

Increasing the air gap of the solid plate as in Figure 6 can be seen to shift the effect of the resonance to lower frequency. The improvement at the resonance due the MPP is the same.

3.2. STL improvement

For clarity of analysis, it is of interest to quantify the level of improvement of the STL which is the dB difference after and before inserting the MPP to the double-leaf. This is also the same as the ratio of the transmitted sound power (represented by the power transmission coefficient) before (τ_b) to after (τ_a) the MPP insertion in dB unit which is given by

$$\Omega = 10\log_{10}\left(\frac{\tau_b}{\tau_a}\right) = \mathrm{STL}_a - \mathrm{STL}_b \tag{34}$$

where STL_a is the transmission loss of the DL-MPP and STL_b is for the DL.

Figure 7 presents the STL improvement, Ω of the DL-MPP system from results in Figures 3, 4, 5 and 6 plotted up to 5 kHz to give clarity at high frequencies. In Figure 7(a), it can be seen that Ω can be achieved up to nearly 10 dB at the resonance for the MPP at $l = 0.1D$ from the solid plate. These results also show that significant improvement of 5 dB or more can be achieved for hole diameter of 2 mm or less. At higher frequency above the resonance, Ω increases rapidly with frequency by more than 20 dB/decade resembling the 'mass-law' trend.

Figure 7(b) shows that smaller hole is preferred for good Ω. This could add the cost to the system as panel with smaller micro holes are more difficult to fabricate. However, this can be compromised with minimum perforation ratio as shown in Figure 7(c) where almost no further improvement is given to Ω around the resonance by varying the perforation ratio. Again the effect can only be seen above the resonance at high frequency (in this case above 70 Hz) where small perforation ratio provides greater Ω.

Figure 7(d) shows the shift of the resonance area because of the change of the air gap distance. Different peak level of Ω in the results is due to different air gap D which also results in different distance l of the MPP to the solid panel. It is also interesting to note the deterioration of Ω just after the resonance (indicating by negative Ω) which can be seen to be greater as the air gap distance is increased. As this is due to the effect of the amount of solid part in the panel, this can be reduced by increasing the perforation ratio as shown in Figure 7(c). In this case, large perforation ratio is chosen if this reduction effect cannot be tolerated in the design.

4. Experiment

The experiment to measure the transmission loss of the proposed system was conducted using the impedance tube method where the specimen was located inside the tube and was excited by a

sound field from a loudspeaker. The tube has 50 mm diameter. Two GRAS acoustic microphones 1/2 inch type 40AE were placed before the sample and the other two microphones were after the sample. The recorded signal from the microphones were then processed by a spectrum analyzer LDS Photon. The diagram of the measurement setup is shown in Figure 8.

Three samples were prepared for the experiment where a sample consisted of three solid 1 mm thick and round aluminium plates with diameter of also 50 mm to properly fit inside the impedance tube. The samples were fitted in a sample holder. To hold the plate sample in its position, a light tape was used between the plate perimeter and the holder. This also was to ensure that the whole plate surface can have small movement when it was exposed by a plane wave acoustic loading to closely resemble the model in Figure 1. Use of light tape was to minimise additional mass introduced to the plate. One of the plates was then perforated with sub-millimetric holes having diameter of 0.3 mm, 0.4 mm and 0.5 mm for each sample. The gap between the solid plates is 70 mm and the MPP was located at 5 mm from the back solid plate.

The tube was fed with white noise up to 800 Hz to only focus the analysis at low frequency range where the effect of mass-air-mass resonance occurs (at around 200 Hz). In this frequency range the acoustic loading still have plane waves propagating along the tube. The signal processing technique for the transmission loss employed the wave decomposition method proposed by Salissou and Panneton [15]. This method applies two-load technique, which means it requires two different loadings for the termination conditions for the transmission coefficient formula to be assembled. In this experiment, the loads were made from glass wool and have two different shapes: conical and circular. The former shape is to provide an anechoic termination in the tube.

Figure 9 shows the experimental results of the transmission loss for several hole diameters and perforation ratios. The measurement data is found to only valid from 400 Hz. This is due to the conical termination which is difficult to be anechoic at low frequencies. The reflected waves thus affect the recorded signal. This could be overcome by having a longer tube for the downstream part (i.e. the tube at the transmission region) to give the reflected waves more time to arrive at the microphone. However above 400 Hz, it can be seen that the measurement data shows reasonably good agreement with the theory.

5. Conclusions

The sound transmission loss of a double-leaf partition system inserted with MPP under normal incidence of acoustic loading has been reported. It is found that the MPP insertion reduces the effect of mass-air-mass resonance found in the conventional double-leaf partition at low frequency. However, this is only effective when the MPP distance is less than half of the air gap of the solid panels and improves as it approaches the solid plate. Reducing the size of the hole improves the STL at resonance while varying the perforation ratio gives only small effect. Optimum effect of sound transmission loss improvement can therefore be achieved with small micro-hole diameter and small perforation ratio. At high frequency above the resonance, for any MPP parameters, the STL of the system increases dramatically due to added mass. The experimental result shows good agreement with the theory at the mass law region, but validation at low frequencies need to be improved to observe the phenomenon at the mass-air-mass resonance. Employing the MPP for a multi-layer structure is thus feasible, particularly for the system exposed with predominantly low frequency noise, for example a window system of a control room close to a stamping machine where the sound impinges at normal direction. The proposed model can be used as a design guide.

Acknowledgment

The authors gratefully acknowledge the financial support provided for this research by the Ministry of Higher Education Malaysia (MoHE) under Fundamental Research Grant Scheme No. FRGS/2010/FKM/TK02/3-F0078.

References

[1] F. J. Fahy and P. Gardonio, *Sound and Structural Vibration: Radiation, Transmission and Response*, Academic Press, London, 2nd edition, 2006.

[2] W. C. Tang, H. Cheng and C. F. Ng, Low frequency sound transmission through close-fitting finite sandwich panels, *Applied Acoustics*, 55(1998), 13–30.

[3] J. M. Bravo, J. Sinisterra, A. Uris, J. Llinares and H. Estelles, Influence of air layers and damping layers between gypsum boards on sound transmission, *Applied Acoustics*, 63(2002), 10513–1059.

[4] Q. Mao and S. Pietrzko, Control of sound transmission through double wall partition using optimally tuned Hemholtz resonators, *Applied Acoustics*, 91(2005), 723–731.

[5] Y. Y. Li and L. Cheng, Mechanism of active control of sound transmission through a linked double wall system into an acoustic cavity, *Applied Acoustics*, 69(2008), 614–23.

[6] D. Li, X. Zhang, L. Cheng and G. Yu, Effectiveness of t-shaped acoustic resonators in low-frequency sound transmission control of a finite double-panel partition, *Journal of Sound and Vibration*, 329(2010), 4740–4755.

[7] M. Mahjoob, N. Mohammadi and S. Malakooti, An investigation into the acoustic insulation of tripple-layered panels containing newtonian fluids : Theory and experiment, *Applied Acoustics*, 70(2009), 165–171.

[8] D. Y. Maa, Theory and design of microperforated panel sound absorbing constructions (in Chinese), *Scientia Sinica*, (18)1975, 55–71.

[9] T. Dupont, G. Pavic and B. Laulagnet, Acoustic properties of lightweight micro-perforated plate systems, *Acta Acustica United with Acustica*, 89(2003), 201–212.

[10] M. Toyoda and D. Takahashi, Sound transmission through a microperforated-panel structure with subdivided air cavities, *Journal of The Acoustical Society of America*, 124(2008), 3594–3603.

[11] R. L. Mu, M. Toyoda and D. Takahashi, Sound insulation characteristic of multi-layer structures with a microperforated panel, *Applied Acoustics*, 72(2011), 849–855.

[12] I. Prasetiyo, Investigation of sound transmission in lightweight structures using a waveguide finite element/boundary element approach, PhD Thesis, University of Southampton (2012).

[13] L. E. Kinsler, A. R. Frey, A. B. Coppens and J. V. Sanders, *Fundamentals of Acoustics*, John Wiley and Sons, New York, 4th edition (2000).

[14] D. Takahashi and M. Tanaka, Flexural vibration of perforated plates and porous elastic materials under acoustic loading, *Journal of the Acoustical Society of America*, 112(2002), 1456–1464.

[15] Y. Salissou and R. Panneton, A general wave decomposition formula for the measurement of normal incidence sound transmission loss in impedance tube, *Journal of the Acoustical Society of America*, 125(2009), 2083–2090.

List of Figures

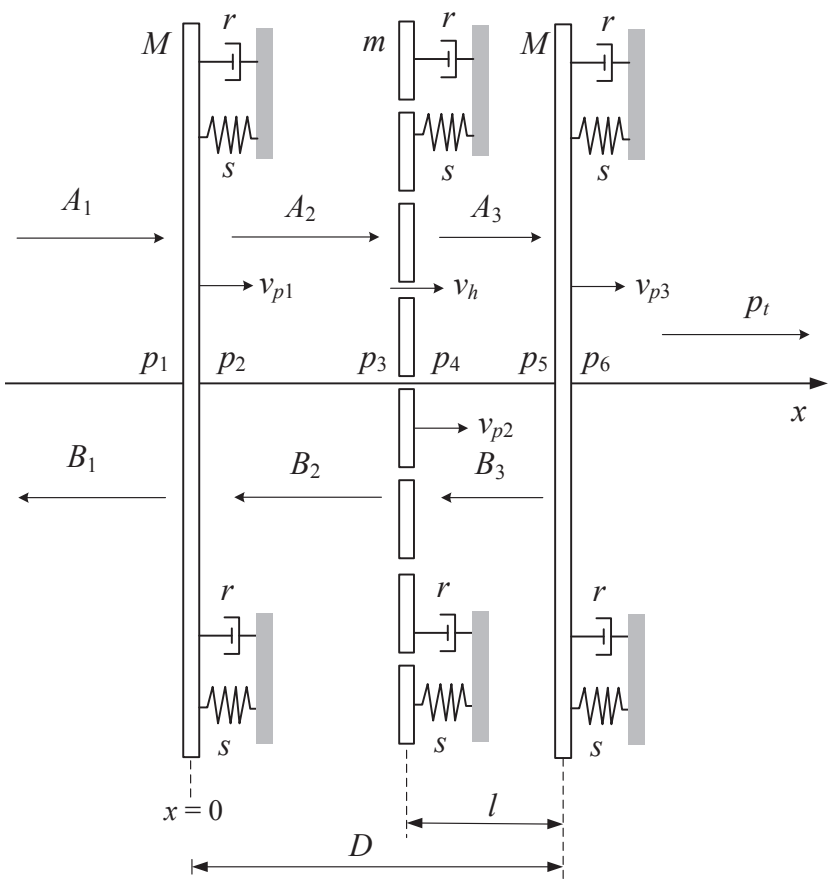

Figure 1: A schematic diagram of a DL-MPP system.

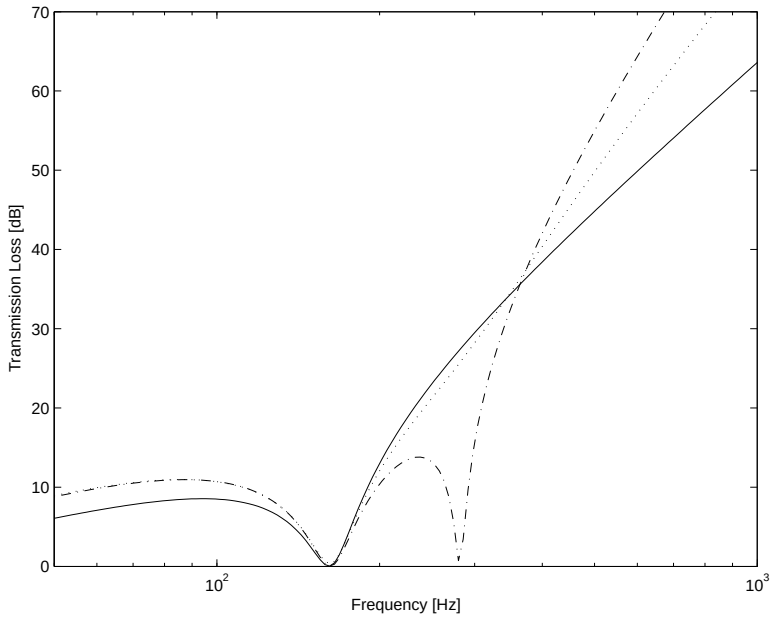

Figure 2: Comparison of sound transmission loss of —DL, $-\cdot-$TL and $\cdots$DL-MPP (aluminium plate: $t = 1$ mm, $D = 100$ mm).

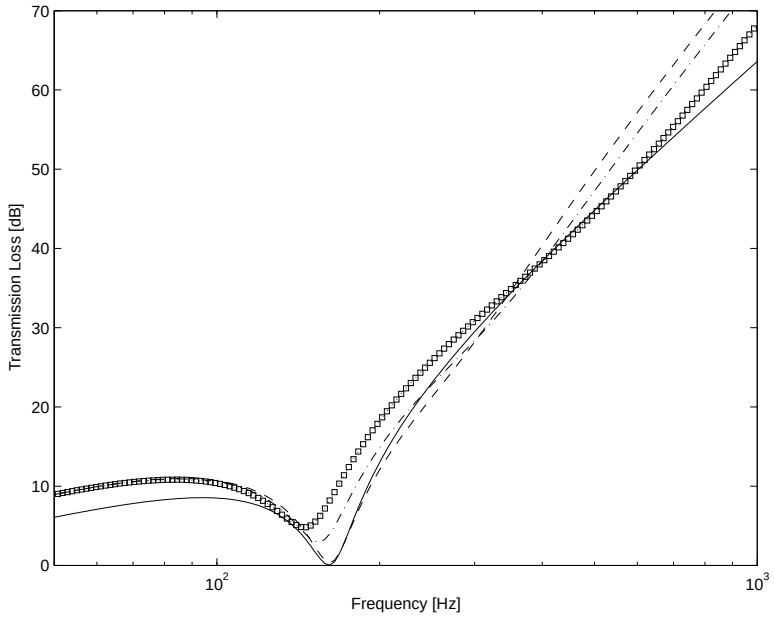

Figure 3: Comparison of sound transmission loss of DL (—) with that of DL-MPP for different locations in the gap ($d_o = 0.1$ mm, $\sigma = 1.5\%$, $D = 100$ mm; $\cdot\Box\cdot\, l = 0.9D$, $--\, l = 0.5D$, $-\cdot-l = 0.2D$, $\cdots l = 0.1D$)

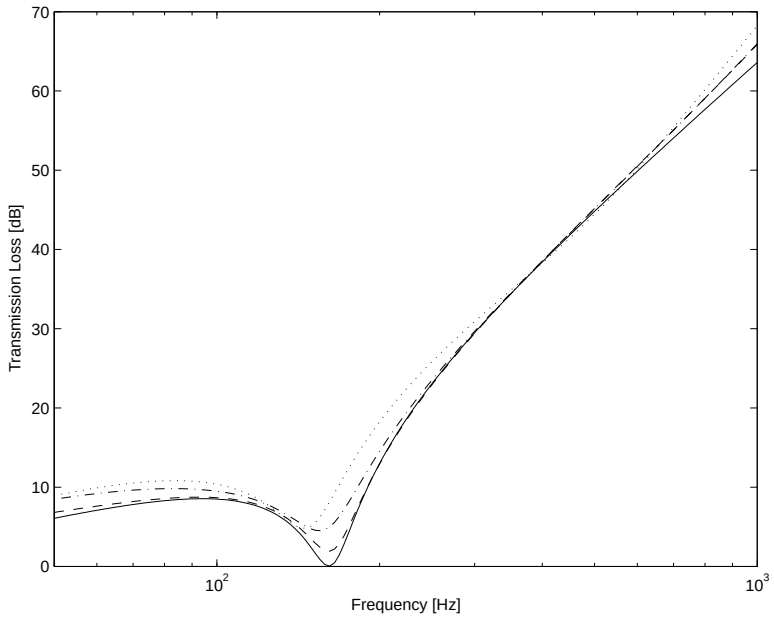

Figure 4: Comparison of sound transmission loss of DL ($-$) with that of DL-MPP for different hole diameters ($l = 0.1D$, σ=1.5%, $D = 100$ mm; $\cdots d_o = 0.1$ mm, $-\cdot- d_o = 0.2$ mm and $--\, d_o = 0.4$ mm)

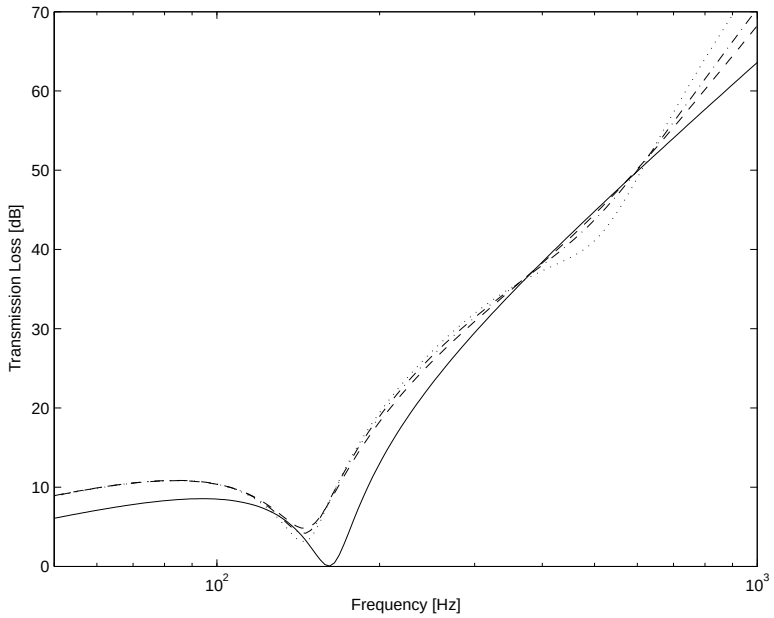

Figure 5: Comparison of sound transmission loss of DL ($-$) with that of DL-MPP for different perforation ratios ($l = 0.1D$, $d_o = 0.1$ mm, $D = 100$ mm; $--\sigma = 0.5\%$, $-\cdot-\sigma = 1.0\%$ and $\cdots\sigma = 1.5\%$)

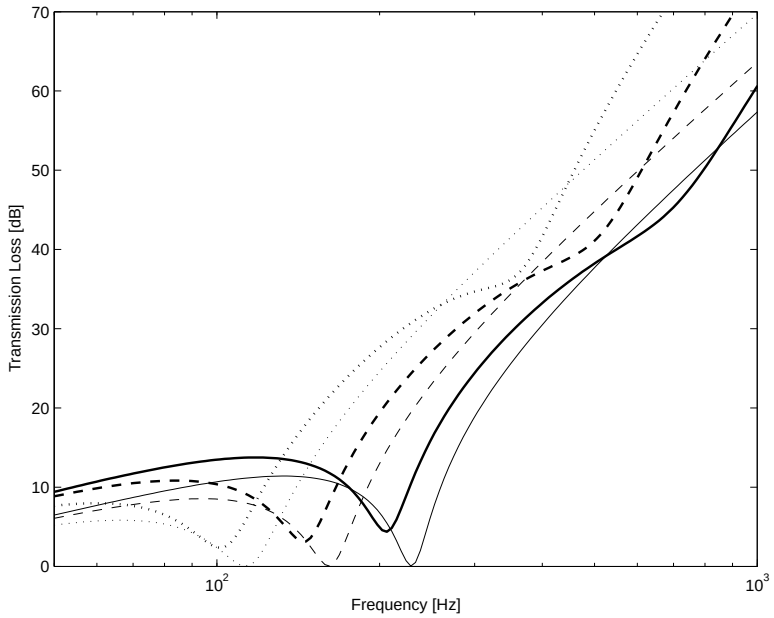

Figure 6: Comparison of sound transmission loss of DL (−) with that of DL-MPP for different air gaps ($l = 0.1D$, $d_o = 0.1$ mm, $\tau = 0.5\%$; —$D = 50$ mm, $--$ $D = 100$ mm and $\cdots$ $D = 200$ mm)

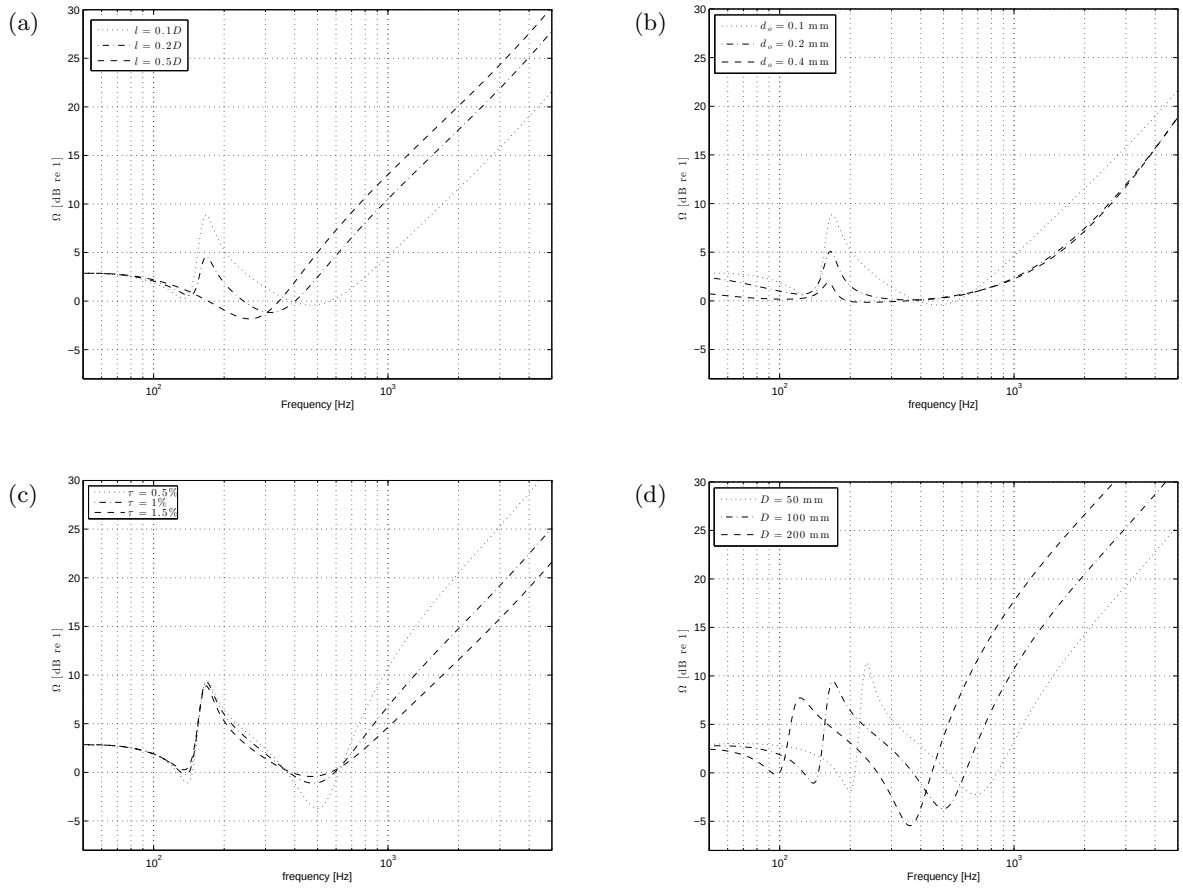

Figure 7: STL improvement of DL-MPP system with different MPP parameters: (a) locations in the gap ($d_o = 1$ mm, $\tau = 1.5\%$, $D = 100$ mm), (b) hole diameters ($l = 0.1D$, $\tau = 1.5\%$, $D = 100$ mm), (c) perforation ratio ($l = 0.1D$, $d_o = 0.1$ mm, $D = 100$ mm) and air gap ($l = 0.1D$, $d_o = 0.1$ mm, $\tau = 1.5\%$).

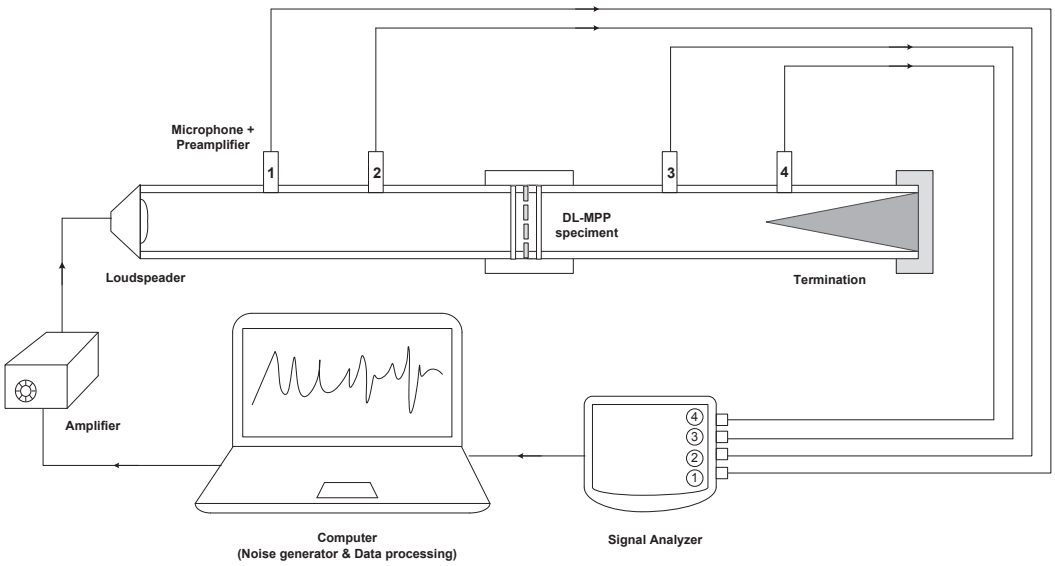

Figure 8: Diagram of the experimental setup for the sound transmission loss measurement.

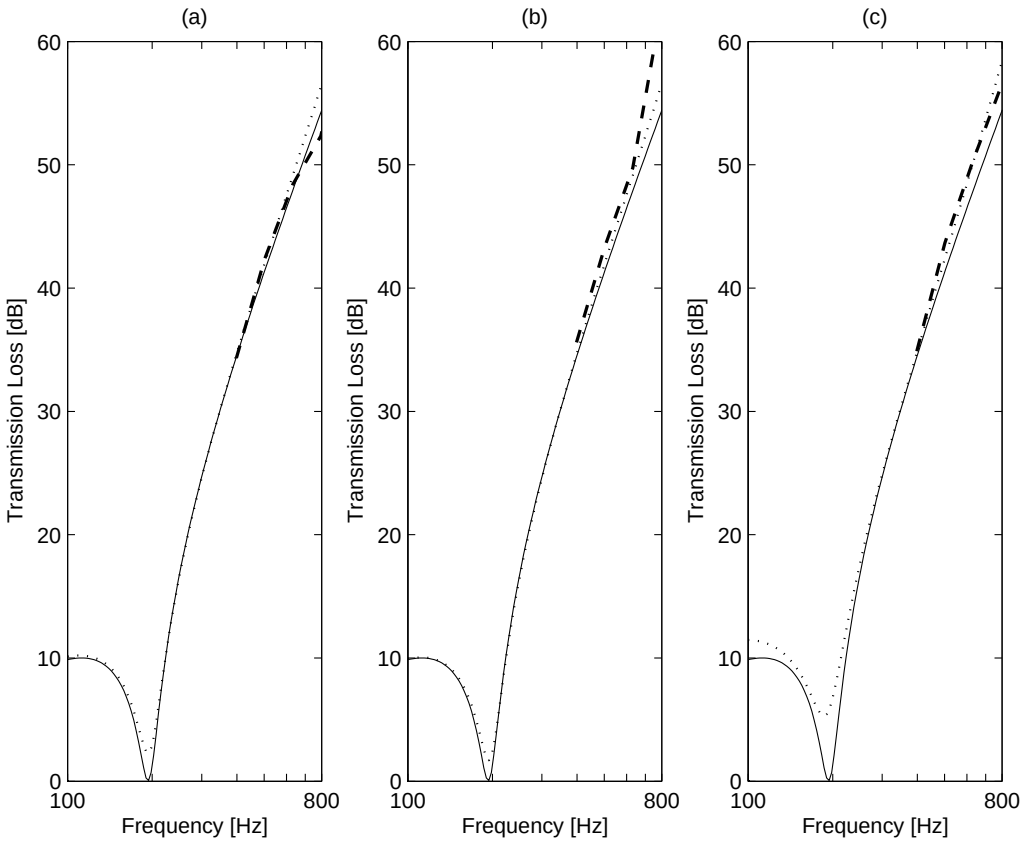

Figure 9: Transmission loss of DLMPP ($D = 70$ mm, $l = 0.15D$): (a) $d_o = 0.3$ mm, $\sigma = 0.5\%$, (b) $d_o = 0.4$ mm, $\sigma = 1\%$ and (c) $d_o = 0.5$ mm, $\sigma = 1\%$ (—theory (double-panel), $\cdots$ theory (DL-MPP), $--$measured).